CHEMISTRY
A EUROPEAN JOURNAL

DOI: 10.1002/chem.200800136

Cyclophanes of Perylene Tetracarboxylic Diimide with Different Substituents at Bay Positions

Junqian Feng, Yuexing Zhang, Chuntao Zhao, Renjie Li, Wei Xu, Xiyou Li,* and Jianzhuang Jiang[a]

Abstract: Cyclophanes of perylene tetracarboxylic diimides (PDIs) with different substituents at the bay positions, namely four phenoxy groups at the 1,7-positions (**1**), four piperidinyl groups at the 1,7-positions (**2**), and eight phenoxy groups at the 1,6,7,12-positions (**3**) of the two PDI rings, have been synthesized by the condensation of perylene dianhydride with amine in a dilute solution. These novel cyclophanes were characterized by ^{1}H NMR spectroscopy, MALDI-TOF mass spectrometry, electronic absorption spectroscopy, and elemental analysis. The conformational isomers of cyclophanes substituted with four piperidinyl groups at the 1,7-positions (**2a** and **2b**) were successfully separated by preparative TLC. The main absorption band of the cyclophanes shifts significantly to the higher energy side in comparison with their monomeric counterparts, which indicates significant π–π interaction between the PDI units in the cyclophanes. Nevertheless, both the electronic absorption and fluorescence spectra of the cyclophanes were found to change along with the number and nature of the side groups at the bay positions of the PDI ring. Time-dependent DFT calculations on the conformational isomers **2a** and **2b** reproduce well their experimental electronic absorption spectra. Electrochemical studies reveal that the first oxidation and reduction potentials of the PDI ring in the cyclophanes increase significantly compared with those of the corresponding monomeric counterparts, in line with the change in the energy of the HOMO and LUMO according to the theoretical calculations.

Keywords: cyclophanes · dimers · perylenes · photophysical properties · supramolecular chemistry

Introduction

Spontaneous self-organization of organic chromophores has been a very active field in supramolecular chemistry since the important role of the chlorophyll aggregates in photosynthesis in purple bacteria was revealed.[1–6] Various supramolecular systems constructed from organic dyes including porphyrins[7] and phthalocyanines[8] based on noncovalent intermolecular interactions, such as hydrogen bonding, metal coordination, dipole–dipole, electrostatic, and π–π interactions, have been intensively studied.[9] However, investigation towards understanding the relationship between structure and spectroscopic as well as electrochemical properties has been retarded because of the flexible supramolecular structures formed based on weak intermolecular interactions. To investigate the dependence of the optical properties on the structure of supramolecular systems, the design and synthesis of model systems with the chromophores bonded into a rigid structure are necessary.

Perylene tetracarboxylic diimides (PDIs) have attracted significant research interest because of their great application potential in field-effect transistors,[10] solar cells,[11] and light-emitting diodes.[12] One fascinating feature of this kind of organic dye is the significant change in the relative intensity of the 0→0 and 0→1 vibronic bands in the absorption spectrum upon π–π stacking, which makes them the ideal model for studying the structure–property relationships of supramolecular systems. Wasielewski and co-workers have prepared a PDI dimer linked by a xanthene spacer.[13,14] The resulting dimer showed a significant blueshifted band in its electronic absorption spectrum, which indicates a strong π–π interaction between the two PDI rings with the transition dipole moments parallel to each other. Li and co-workers reported a series of PDI dimers or foldamers linked by long and flexible ethylene oxide or single-stranded DNA.[15] The intensity reversal between the 0→0 and 0→1 vibronic bands

[a] J. Feng, Y. Zhang, C. Zhao, R. Li, W. Xu, Prof. X. Li, Prof. J. Jiang
Key Lab for Colloid and Interface Chemistry of Education Ministry
Department of Chemistry, Shandong University
Jinan 250100 (China)
Fax: (+86) 531-8856-4464
E-mail: xiyouli@sdu.edu.cn

Supporting information for this article is available on the WWW under http://dx.doi.org/10.1002/chem.200800136.

InterScience
© 2008 Wiley-VCH Verlag GmbH & Co. KGaA, Weinheim

in the absorption spectra of these PDI dimers or foldamers upon π–π stacking is solvent dependent, which indicates the change in the molecular geometry of the stacked structure in different solvents. Two PDI units linked by a flexible triazine ring presented an equilibrium between the stacked and unstacked conformation in solution, as revealed by the absorption and emission properties in different solvents.[16] The only cyclized PDI dimer, that is, cyclophane of PDIs, formed by two PDI rings linked by two long and flexible alkyl chains at imide nitrogen atoms showed a conformational change from *H* to *J* aggregate upon photoexcitation, as evidenced by the blueshifted absorption bands and redshifted emission bands.[17] Investigation towards establishing direct correlation between the molecular structure and optical properties for all the above-mentioned PDI dimers is impossible due to their flexible molecular geometry. However, a recent theoretical examination of PDI dimers with a face-to-face stacked molecular structure by using time-dependent density functional theory (TDDFT) clearly revealed the effects of the molecular conformation, including the interplanar distance, lateral slippage along either the N–N axis or the in-plane short axis of PDI, and the rotation of one subunit relative to another, on the optical properties of the PDI dimer.[18]

Herein, we report the design, synthesis, and optical properties of four PDI cyclophanes with different substituents at the bay positions of the PDI ring (Scheme 1, **1**–**3**). Two PDI rings are connected by two 2,4-diamino-1,3,5-triazine rings and form a rigid cyclic structure. The difference in the number and species of side groups attached at the bay positions of the PDI rings in these cyclophanes induces different degrees of slipping and/or rotation of the two PDI rings relative to each other. The electronic absorption and fluorescence spectroscopic results for the series of compounds are revealed to depend on the geometry of the stacked structure, which is also confirmed by the results calculated by the TDDFT method. To the best of our knowledge, this represents the first experimental effort towards constructing the structure–property relationship for the face-to-face stacked PDI dimer.

Results and Discussion

Molecular design and synthesis: To prepare a PDI dimer with rigid structure and efficient π–π interactions between the PDI rings, the spacer used to connect the PDI subunits must be able to confine the two PDI rings in a parallel way and keep the two subunits at a proper distance. 2,4-Diamino-1,3,5-triazine has been proved an ideal bridge for this purpose on the basis of our previous research.[16] Therefore, 2,4-diamino-1,3,5-triazine was chosen as the spacer to connect two PDI rings for this cyclophane compound. It has been revealed that introducing substituents at the bay positions of the PDI ring is an effective way to tune the optical and electrochemical properties of PDI compounds.[19] Therefore, different numbers of phenoxy or piperidinyl groups are incorporated into the bay positions of PDI rings. In addition, introduction of side groups onto the PDI rings significantly improves the solubility of cyclophanes in conventional organic solvents, which simplifies the preparation and purification procedure to a large degree.

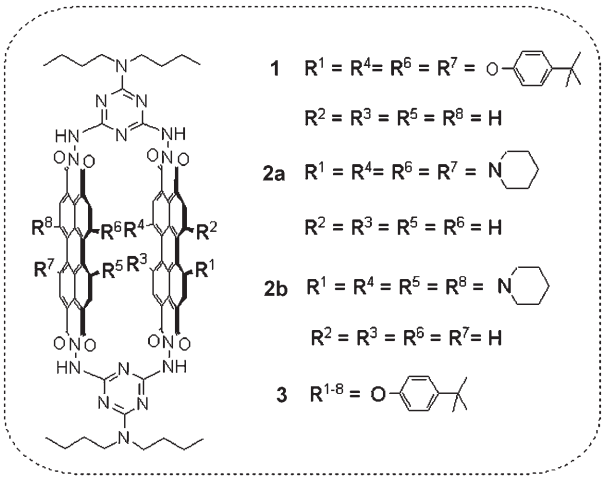

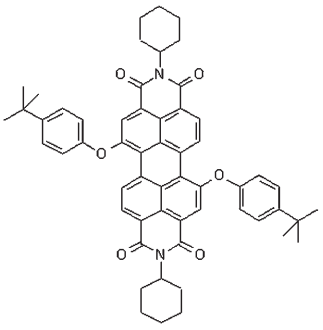
4

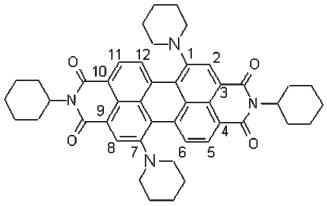
5

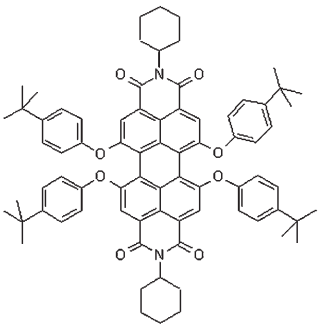
6

Scheme 1. Molecular structure of cyclophanes **1**–**3** and the reference compounds **4**–**6**. Labels of the carbon atoms on the PDI ring are shown on the structure of **5**.

Condensation of substituted perylene tetracarboxylic dianhydrides (**8**–**10**) with 2-*N*,*N*-di(*n*-butyl)amino-4,6-dihydrazine-1,3,5-trazine (**7**) in toluene in the presence of imidazole leads to the formation of cyclophanes (Scheme 2). Note that a dilute solution is employed in the reaction to prevent polymerization.[20] Target cyclophane compounds were purified by column chromatography and/or preparative TLC.

The reaction of 1,7-di(4-*tert*-butylphenoxy)perylene-3,4:9,10-tetracarboxylic dianhydride (**8**) or 1,7-dipiperidinylperylene-3,4:9,10-tetracarboxylic dianhydride (**9**) with **7** induces the formation of two conformational

 © 2008 Wiley-VCH Verlag GmbH & Co. KGaA, Weinheim

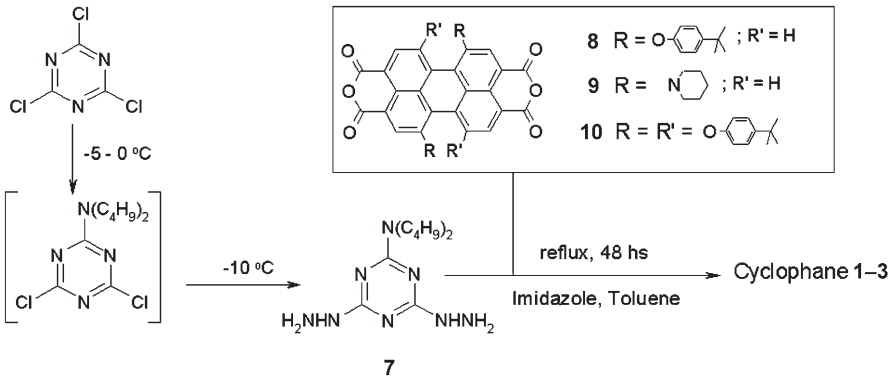

Scheme 2. Synthesis of the cyclophanes **1**–**3**.

isomers for cyclophanes **1** and **2** because of the blocked rotation of the disubstituted perylene ring along the long molecular axis. We have indeed isolated a product from the reaction mixture during the preparation of compound **1**, which gives a molecular mass corresponding well with the dimeric structure. However, observation of two sets of proton signals in its ^{1}H NMR spectrum (see Figure S1 in the Supporting Information) indicates the presence of two isomers with one as the main product. The mole ratio calculated from the integral of the peaks for the protons at position 5 is 5:2 for the two isomers. However, attempts to separate these two isomers by various chromatographic methods have been unsuccessful.

Fortunately, the isomers **2a** and **2b** (Scheme 3) have been successfully separated by preparative TLC in the mole ratio of 3:1. The first component is the main product, cyclophane **2a**, which easily dissolves in most common organic solvents. In contrast, the second isomer separated with low yield, cyclophane **2b**, is hard to dissolve in organic solvents in comparison with **2a**. As expected, the two isomers give identical mass but different ^{1}H NMR spectra (see Figures S2 and S3 in the Supporting Information). To identify the molecular structure, 2D COSY and ROESY NMR spectra for both isomers were recorded in $CDCl_3$. For the purpose of comparison, the 2D ROESY NMR spectrum of a monomeric PDI, namely *N*,*N*′-di-*n*-butyl-1,7-dipiperidinyl-3,4:9,10-tetracarboxylic diimide (**11**), was also recorded. Figure 1 shows the 2D ROESY spectrum of **2a**. A cross peak corresponding to the correlation between the protons at positions 5 and 2 as well as the protons at positions 11 and 8 of the PDI rings appears in this spectrum. However, a similar correlation signal was not observed in the 2D ROESY of monomeric PDI **11** (see Figure S5 in the Supporting Information). As a consequence, the cross peak in cyclophane **2a** should result from the correlation between the protons at position 5 of one PDI ring and position 2 of another PDI ring as well as between the protons at position 8 of one PDI ring and position 11 of the other PDI unit, which also suggests a *trans* configuration for the two PDI units. In addition, five signals indicating the correlations of the protons at positions 5 and 11 of the PDI rings with those on piperidinyl rings were also observed in the 2D ROESY spectrum of **2a** (Figure 1). Comparison with the correlation signals in the 2D ROESY spectrum of monomeric compound **11** (see Figure S5 in the Supporting Information) indicates that these five signals are due to the correlations of the protons at positions 5 and/or 11 of the PDI ring with those protons on the piperidinyl rings connected at the same PDI ring, as well as the protons of piperidinyl rings connected on the other PDI ring. These results give additional support to the *trans* configuration of the PDI units in cyclophane **2a**. Note that in the 2D ROESY spectrum of the *cis* isomer **2b** (see Figure S8 in the Supporting Information), correlation of the protons at positions 2 and 8 of the PDI ring with the protons of its own piperidinyl substituent was also observed, as in its *trans* isomer **2a**. However, unlike the *trans* isomer, the PDI proton at position 5 (or 11) of the PDI ring can only correlate with one of the two protons neighboring the nitrogen atom in the piperidinyl groups attached to this PDI ring in the *cis* isomer **2b**. These results indicate a large repulsion between the two piperidinyl groups attached to two different PDI rings in cyclophane **2b**, which forces the piperidinyl groups to bend away from the plane of the PDI rings and therefore suggests a *cis* configuration for the PDI units in this isomer.

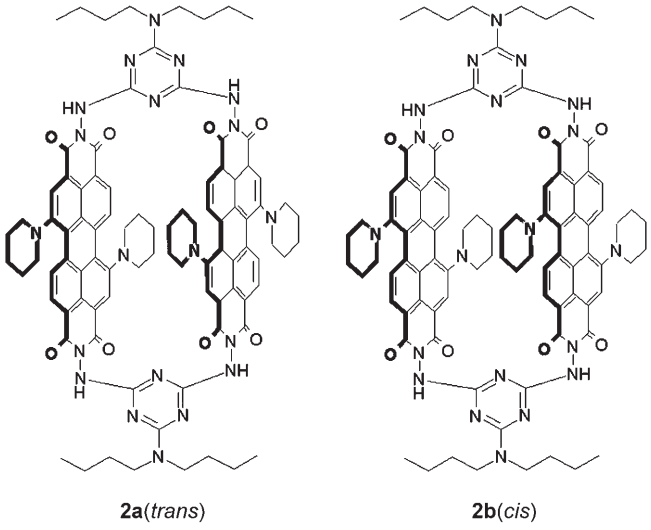

Scheme 3. Molecular structure of *trans* and *cis* isomers of cyclophane **2**.

Reaction between 1,6,7,12-tetra(*p*-*tert*-butylphenoxyl)perylene-3,4:9,10-tetracarboxylic dianhydride (**10**) and 2-di(*n*-butyl)amino-4,6-dihydrazine-1,3,5-triazine (**7**) leads to the isolation of cyclophane **3** in very low yield (3.1 %), probably due to the large steric hindrance between the eight bulky phenoxy groups attached at two different PDI rings. This is

 © 2008 Wiley-VCH Verlag GmbH & Co. KGaA, Weinheim

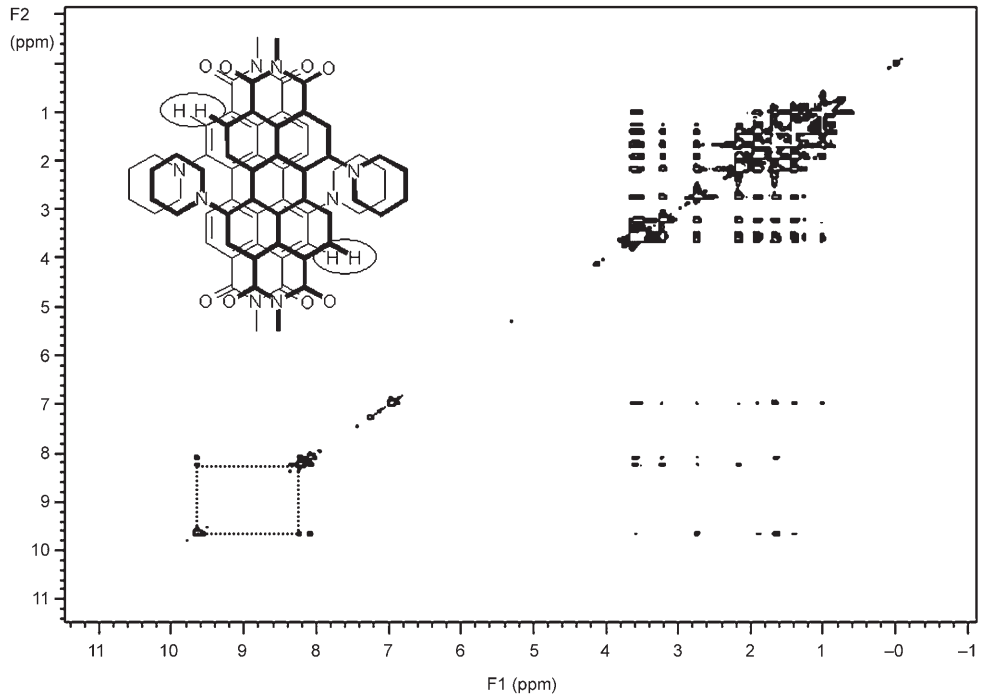

Figure 1. 2D ROESY NMR spectrum of cyclophane **2a** in $CDCl_3$ at room temperature. Inset: correlation of the protons at positions 5 and 11 of one of the PDI units to those at positions 2 and 8 of the other unit.

rationalized by the fact revealed previously that all the 1,6,7,12-tetrasubstituted PDI compounds form *J* aggregates exclusively in their self-assembly.[21] Interestingly, broad peaks without fine structure were observed in the ^{1}H NMR spectrum of cyclophane **3** (see Figure S4 in the Supporting Information), which indicates the restricted rotation of the phenoxy groups along the O–C bond with a rate comparable to the response of the NMR instrument due to the large steric hindrance among the phenoxy groups.

Minimized structure: The minimized structures of these cyclophanes have been calculated by the B3LYP method and 6-31G(d) basis set in the Gaussian 03 program.[22] The structure of cyclophane **2b** is shown in Figure 2 as a representative example. The calculated structures of other cyclophanes are shown in Figure S9 in the Supporting Information. As can be seen, in these cyclophanes the two triazine spacers connect two PDI rings to form a cyclic rigid molecule in which the two PDI rings employ a face-to-face stacked structure. All the structure parameters, including the interplanar distance between the two PDI planes (d_1), the sideways slippage along the long axis of the PDI ring (d_2), the slippage along the short axis of the PDI ring (d_3), the in-plane torsion angle between the long axis of the two PDI rings (α), and the dihedral between the PDI planes (β), were calculated for both isomers of **1** and **2** together with cyclophane **3** and the data are summarized in Table 1.

All the parameters except d_1 for the *trans* isomer **1a** are close to zero (Table 1), thus indicating an ideal face-to-face stacking for the two PDI units without any sideways slipping

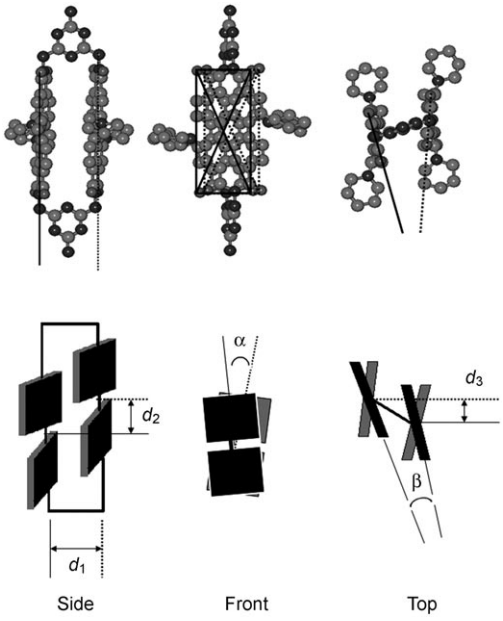

Figure 2. Top: The minimized structure of cyclophane **2b** (hydrogen atoms are omitted for clarity). Bottom: a schematic description of the structure parameters.

or in-plane torsion of the PDI rings relative to each other. However, in addition to the interplanar distance between the two PDI planes, the in-plane torsion angle between the long axis of the two PDI rings for the *cis* isomer **1b** is no longer zero. These results indicate a structure with zero side-

 © 2008 Wiley-VCH Verlag GmbH & Co. KGaA, Weinheim

Table 1. Parameters of the dimeric structure of PDI in cyclophanes **1–3**.

Compound	d_1[a] [Å]	d_2[b] [Å]	d_3[b] [Å]	α [°]	β [°]
1a	4.81	0	0.35	0	0
1b	4.85	0	0	15.38	0
2a	4.56	0	1.25	6.06	0
2b	4.46	0	1.61	0	14.96
3	4.77	0.72	1.80	8.11	14.70

[a] Four atoms (two imide nitrogen and 1,7-carbon) are selected in one PDI ring and the distance from the selected atoms to their projections on the opposite PDI ring are measured. The interplanar distance d_1 was calculated from the average of these four measured distances. [b] The slippage was measured at the molecule center (the cross point of the diagonals of the rectangle that links the four imide oxygen atoms in one PDI ring).

ways slippage along both the short and long axes for the PDI rings, and a parallel conformation between the two PDI planes but distinct rotation of the PDI rings relative to each other for the *cis* isomer. Furthermore, the calculated results indicate a smaller energy of the minimized structure for isomer **1a** in comparison with isomer **1b**, which suggests that the *trans* isomer **1a** is more thermodynamically preferred. This is also true for the two isomers of cyclophane **2**. It is therefore reasonable to assign the dominant isomer of cyclophane **1** as *trans* isomer **1a**. This result is further rationalized by the much higher yield of *trans* isomer **2a** than *cis* isomer **2b**, as described above.

For both the *trans* **2a** and *cis* **2b** isomers, the sideways slippage along the long axis of the PDI ring is calculated to be 0 Å, which indicates no sideways slipping along the long axis of the PDI rings (Table 1). In contrast, the large value of d_3 of 1.25 and 1.61 Å for **2a** and **2b**, respectively, reveals noticeable sideways slipping along the short axis of the PDI rings in these two isomers. Notably, the relatively smaller value of d_3 for the *trans* isomer **2a** in comparison with that for the *cis* isomer **2b** suggests a relatively more intense interaction between the two PDI rings in the former isomer, if only in terms of the sideways slippage along the short axis of the PDI ring.[18] However, both the larger values of the interplanar distance between the two PDI planes (d_1) and the in-plane torsion angle between the long axis of the two PDI rings (α) for the *trans* isomer **2a** relative to those of *cis* isomer **2b** appear to induce weaker interaction between the two PDI rings in the *trans* isomer. Additionally, contrary to the two parallel PDI rings in the *trans* isomer **2a**, a nonparallel stacking of PDI rings was employed by the *cis* isomer **2b** with a dihedral of 14.96°.

As expected, eight bulky phenoxy groups attached to the bay positions of the PDI rings in cyclophane **3** lead to significant distortion over the PDI rings in the molecular structure due to the large steric hindrance among the phenoxy groups. The calculated results summarized in Table 1 reveal that both the long and short axes of the PDI rings are not parallel to each other again in this cyclophane. The large value of the sideways slippages along the long and short axes of the PDI ring (d_2 and d_3), the distinct in-plane torsion angle of the two PDI rings (α), and the nonparallel conformation between the two PDI planes (β) for this compound indicate weakened interaction between its two PDI rings.

The UV/Vis absorption spectra: Figure 3 compares the electronic absorption spectra of cyclophanes **1–3** with those of their monomeric counterparts **4–6** in dichloromethane. All the main absorption bands of cyclophanes **1–3** are blueshifted relative to those of their monomeric counterparts **4–6**, which confirms the face-to-face stacked molecular geometry between the two PDI rings in these cyclophane compounds.[23] In particular, cyclophane **3** appears to represent the first example of a PDI dimeric structure in which the two tetra(phenoxy)-substituted PDI rings form a face-to-face geometry.

As shown in Figure 3A, cyclophane **1** (actually the mixture of the two isomers **1a** and **1b**) presents a maximal absorption band at 512 nm, which corresponds to the transition to the allowed higher-energy exciton-split LUMO of perylene. Different from other PDI dimers constructed from two PDI rings connected by a soft or rigid spacer,[13,24] the absorption due to the formally disallowed transition to the lower-energy exciton-split LUMO of perylene at approximately 550 nm is almost negligible. Note that for the face-to-face stacked PDI dimeric system, the transition to the higher-energy exciton-split LUMO of perylene should have the whole oscillator strength, whereas the transition to the lower-energy exciton-split LUMO is symmetry forbidden according to exciton theory. However, the latter transition with significant oscillator strength is always observed in the recorded electronic absorption spectra of dimeric PDI systems reported thus far. This finding has been explained on the basis of vibronic coupling in the exciton states of the dimeric systems, which relieves the symmetry restriction to the transition to the lower-energy exciton-spilt LUMO according to the simple exciton model.[25] The negligible band corresponding to the transition to the lower-energy exciton-split LUMO in the electronic absorption spectrum of cyclophane **1** can be attributed to the strictly face-to-face stacked structure in both *trans* isomer **1a** and *cis* isomer **1b** as detailed above, which efficiently reduces the vibronic coupling in the exciton states of cyclophane **1**.

The main absorption band for the cyclophane *trans* isomer **2a** and *cis* isomer **2b** appears at 632 and 617 nm, respectively, which is blueshifted by about 40 and 55 nm, respectively, compared with that of their monomeric counterpart **5**. This agrees well with previous results on other PDI dimeric systems.[14] In particular, the different blueshift of the main absorption band for isomers **2a** and **2b** compared with that of their monomeric counterpart **5** indicates different π–π interaction strength between the two PDI rings, associated with the difference in the molecular structure of these two isomers. To understand the difference in the electronic absorption spectra of the *trans* isomer **2a** and *cis* isomer **2b**, their frontier orbitals were calculated by DFT. Figure 4 displays the frontier molecular orbital maps together with their energy levels for isomers **2a** and **2b**. As can be seen, the HOMO−1, HOMO, LUMO, and LUMO+1 of

 © 2008 Wiley-VCH Verlag GmbH & Co. KGaA, Weinheim

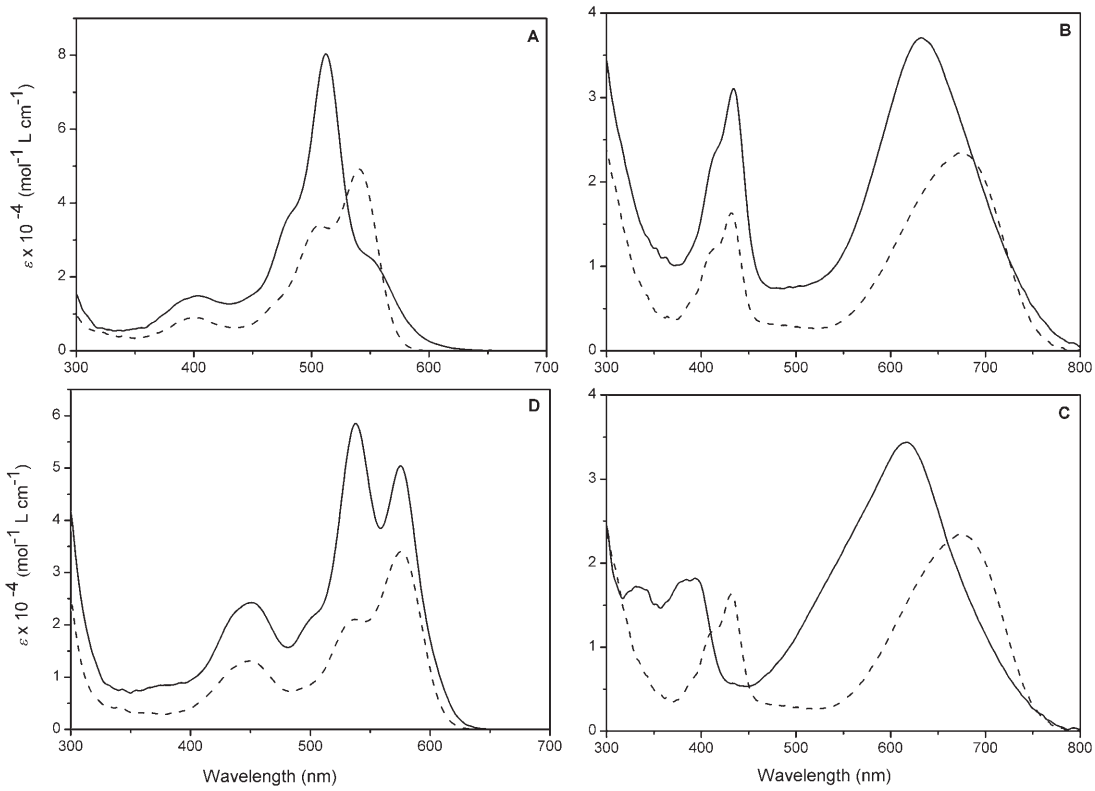

Figure 3. Absorption spectra of cyclophanes **1** (A), **2a** (B), **2b** (C), and **3** (D) (——) and of their monomeric counterparts **4**–**6** (-----) in dichloromethane at room temperature. The spectra were recorded at a concentration of 1×10^{-5} mol L^{-1} for all compounds.

trans isomer **2a** are distributed equally on both PDI units, with HOMO−1 as the bonding orbital and HOMO the antibonding orbital. The extremely small energy splitting between HOMO−1 and HOMO (0.004 eV) and between LUMO and LUMO+1 (0.021 eV) indicates relatively small interaction between the two PDI units in the *trans* isomer **2a**. However, calculations revealed that the HOMO−1 and LUMO are distributed on one of the two PDI units, whereas the HOMO and LUMO+1 are on the other unit for the *cis* isomer **2b**. As a consequence, the energy splitting between both HOMO−1 and HOMO and between LUMO and LUMO+1 for the *cis* isomer **2b** (0.135 and 0.174 eV, respectively) is significantly larger than that for the *trans* isomer **2a**, thus indicating the intensified π–π interaction between the two PDI units in the *cis* isomer **2b**. As mentioned above, the interaction between the two PDI rings in cyclophane is determined by five factors. In the present case, the smaller interplanar distance between the two PDI planes (d_1) and the smaller in-plane torsion angle between the long axes of the two PDI rings (α) for the *cis* isomer **2b** seem to be responsible for the relatively stronger π–π interaction between the two PDI rings compared with that in the *trans* isomer **2a**, despite the larger sideways slippage along the short axis of the PDI ring (d_3).

Figure 5 shows the simulated electronic absorption spectra for isomers **2a** and **2b**. In good consistency with the experimental results, our calculated results show that the lowest-energy absorption at 632 nm, due to the electronic transitions from HOMO to LUMO+1 and from HOMO−1 to LUMO, for *trans* isomer **2a** appears at the lower-energy side of the *cis* isomer **2b** at 625 nm. This result is also in line with the relatively larger blueshift observed for the main absorption band of the *cis* isomer **2b** in comparison with that of the *trans* isomer **2a**, as detailed above.

The main absorption band for cyclophane **3** was observed at 537 nm (Figure 3D), which is blueshifted by about 40 nm compared with its monomeric counterpart, thus indicating the face-to-face geometry for the two PDI rings in this cyclophane. Different from cyclophanes **1** and **2**, an obvious absorption at 575 nm corresponding to the transition to the lower-energy exciton-split LUMO was found in the electronic absorption spectrum of cyclophane **3**. This result suggests weaker π–π interaction between the two PDI rings in **3** than in **1** and **2** because of the large degree of deviation from the ideal face-to-face stacking geometry for the two PDI units in cyclophane **3**. This promotes the vibronic coupling in the exciton states and relieves the symmetry restriction to the transition to the lower-energy exciton-split LUMO of perylene, according to the simple exciton model.

Fluorescence spectra and fluorescence lifetime: The fluorescence spectra of cyclophanes **1**–**3** in different organic solvents were recorded and the fluorescence quantum yields (Φ_f) were calculated with their monomeric counterparts as standards. In addition, the fluorescence lifetimes (τ) were measured by a phase modulation method with a scattering

 © 2008 Wiley-VCH Verlag GmbH & Co. KGaA, Weinheim

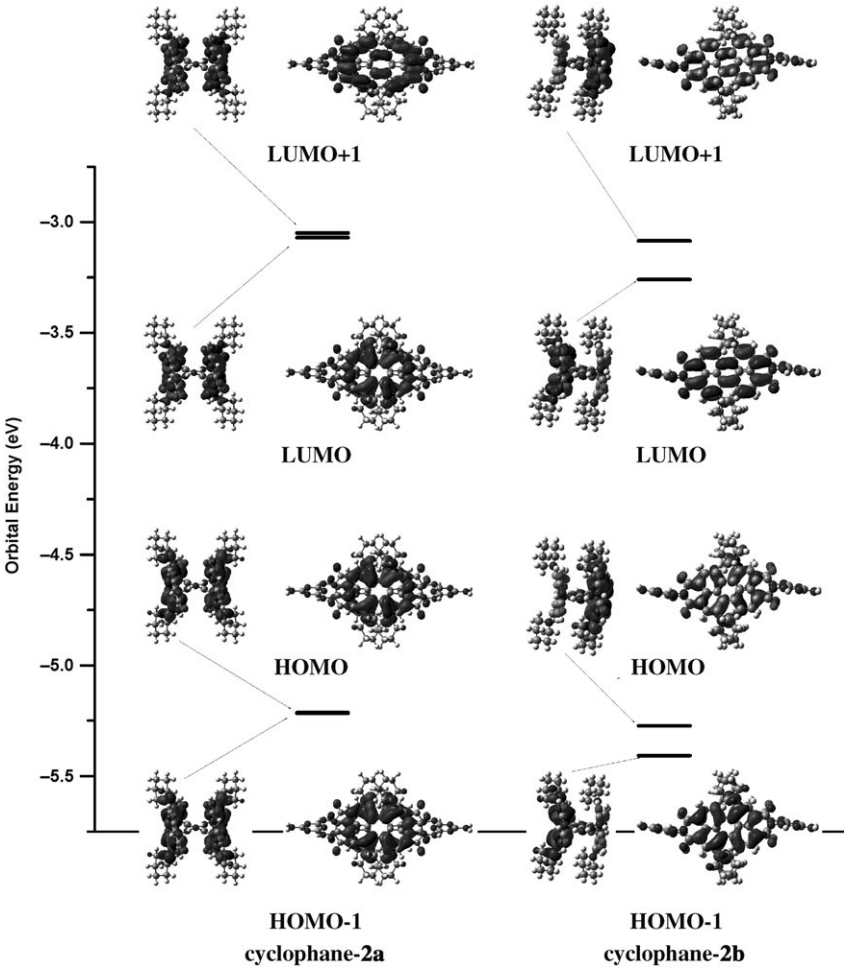

Figure 4. Frontier orbital maps and energy levels of isomers **2a** (left) and **2b** (right) calculated by DFT.

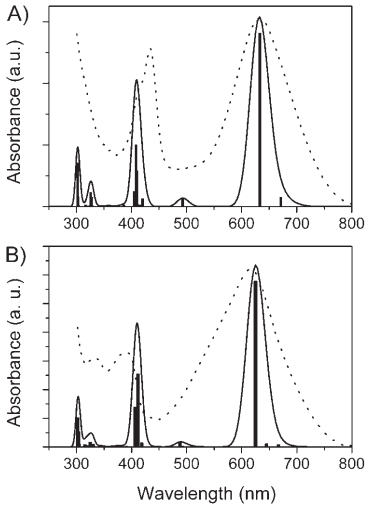

Figure 5. Simulated (——) and experimental (-----) absorption spectra of cyclophanes **2a** (A) and **2b** (B) in chloroform. Bars indicate the contribution modes.

solution as reference. The fluorescence spectra of cyclophanes **1** and **3** are shown in Figure 6 and the fluorescence quantum yields and lifetimes are summarized in Table 2. Notably, no emission was detected for either of the two isomers of cyclophane **2**, which indicates the presence of charge separation between the two PDI units in this compound, as observed previously by Wasielweski in a noncyclic PDI dimer.[14]

As shown in Figure 6, an intense emission band at 659 nm appears in the fluorescence spectrum of cyclophane **1** recorded in CH_2Cl_2, which shifts to the lower-energy direction by about 90 nm in comparison with that of the monomeric counterpart **4**. This broad, structureless band is attributed to the excimer's emission according to previous reports.[13,23] Comparison of the results shown in Table 2 reveals that the fluorescence quantum yields of cyclophane **1** in organic solvents are significantly smaller than those of the monomeric counterpart **4**, which meanwhile decrease along with an increase in the polarity of the organic solvent. These results suggest that the excited states of cyclophane **1** have a remarkable electron-transfer characteristic, which induces a mass of nonradioactive decay of the excited states and in turn leads to a significant decrease in the fluorescence quantum yields. In addition, the fluorescence lifetime of cyclophane **1** also shows dependence on the polarity of the solvents due to the different stabilization ability of solvents with different polarity to the excited states.[24] Interestingly, the fluorescence lifetime of cyclophane **1** in toluene, 38.1 ns, is significantly longer than that of other PDI dimers connected by a spacer with a flexible structure in the same solvent,[13,16] most probably due to the rigid molecular structure of both *trans* and *cis* isomers of cyclophane **1** which hinders structural relaxation during the decay of the excited states. In addition, this is the longest fluorescence lifetime observed so far for a face-to-face stacked PDI dimer.

Similar to its monomeric counterpart **6**, the emission of cyclophane **3** appears at 605 nm (Figure 6B). However, the fluorescence lifetime of cyclophane **3** decreases along with an increase in the polarity of the solvent, in line with the results for cyclophane **1**. This is obviously different from the

 © 2008 Wiley-VCH Verlag GmbH & Co. KGaA, Weinheim

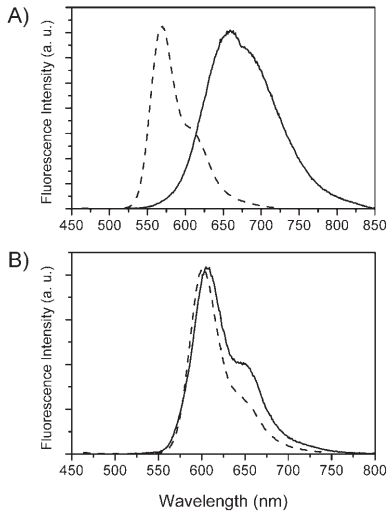

Figure 6. Fluorescence spectra of cyclophanes **1** (A) and **3** (B) (——) compared with those of compounds **4** (A) and **6** (B) (-----) in dichloromethane (excited at 400 nm).

Table 2. Photophysical properties of compounds **1–6**.

Compound	λ_{abs} [nm]	λ_{em} [nm]	Φ_f [%]			τ [ns]		
			toluene	THF	CH_2Cl_2	toluene	THF	CH_2Cl_2
1	512	660	5.53	1.45	1.10	38.09	15.38	13.25
2a	632	–	–	–	–	–	–	–
2b	617	–	–	–	–	–	–	–
3	537	605	5.51	1.32	0.89	11.36	3.85	2.39
4	540	569	100	100	100	4.63	4.69	4.64
5	672	730	3.41	1.35	6.8	3.64	1.97	2.46
6	576	602	81.2	82.0	80.1	6.19	6.80	6.78

behavior of its monomeric counterpart **6**, which shows an almost unchanged fluorescence lifetime at approximately 6.80 ns in different solvents. More importantly, analysis of the fluorescence characteristics of cyclophane **3** in all three solvents reveals a single exponential decay for the excited states of this compound, and no component close to the fluorescence lifetime of monomeric counterpart **6** is observed. All these results indicate the dimeric-structure-originated nature of the emission at 605 nm for cyclophane **3**, despite the similar emission wavelength to its monomeric counterpart.

Electrochemistry: The electrochemical behavior of all the newly synthesized cyclophanes was investigated by cyclic voltammetry (CV) and differential pulse voltammetry (DPV) in CH_2Cl_2. The half-wave redox potential values versus SCE for cyclophanes **1–3** and their monomeric counterparts **4–6** are summarized in Table 3. Figure 7 shows the cyclic and differential pulse voltammograms of cyclophane **2a** as a typical representative of the series of compounds. Within the electrochemical window of CH_2Cl_2, cyclophanes **1–3** undergo at least one reversible one-electron oxidation process and two quasi-reversible one-electron reductions.

Table 3. Half-wave redox potentials[a] (vs. SCE) of cyclophanes **1–3** and their monomeric counterparts **4–6** in CH_2Cl_2.

Compounds	Ox_2	Ox_1	Red_1	Red_2	Red_3	$E^o_{1/2}$[b]
1		1.72	−0.55	−0.71		2.27
2a		0.86	−0.66	−0.81	−0.98	1.54
2b		0.9	−0.63	−0.8	−1.06	1.53
3	1.27	1.38	−0.66	−0.85		2.04
4		1.44	−0.67	−0.89		2.11
5		0.79	−0.78	−0.96		1.57
6	1.78	1.28	−0.72	−0.95		2.00

[a] Values obtained by DPV in dry CH_2Cl_2 with 0.1 M tetrabutylammonium phosphate (TBAP) as the supporting electrolyte and Fc/Fc^+ as internal standard. [b] $E^o_{1/2} = Ox_1 - Red_1$.

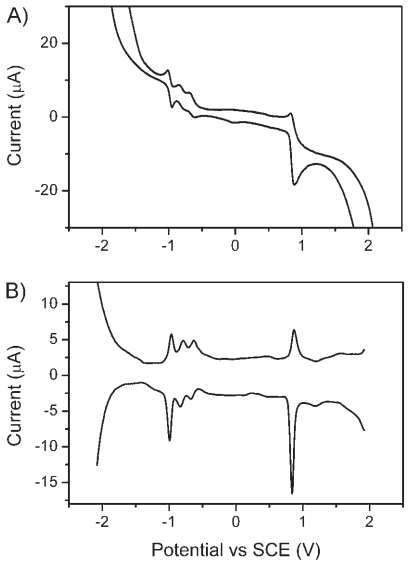

Figure 7. CV (A) and DPV (B) plots of cyclophane **2a** in dichloromethane containing 0.1 M TBAP.

Comparison of the first oxidation and reduction potentials of cyclophane **1** with those of its monomeric counterpart **4** reveals that the face-to-face stacking of the PDI rings shifts the half-wave potentials for the first oxidation and reduction to the positive direction and makes cyclophane **1** harder to oxidize and more easily reduced, which indicates the decrease in the energy of both the HOMO and LUMO of the dimeric cyclophane **1.** A similar positive shift for the first oxidation and reduction potentials of cyclophanes **2** (including both **2a** and **2b**) and **3** compared with their monomeric counterparts **5** and **6**, respectively, is also observed. This finding is in line with DFT calculations on the energy of the frontier molecular orbitals of both *trans* and *cis* isomers of cyclophane **2** (Figure 4). In comparison with the almost identical electrochemical property of the PDI dimer linked by one triazine spacer with a flexible structure,[16] the above-mentioned results reveal the crucial role of the rigid face-to-face stacked geometry in cyclophanes **1–3** for the positive shift of their first oxidation and reduction potentials. Furthermore, the larger positive shift in the first oxidation and reduction potentials for cyclophane **1** relative to its mono-

 © 2008 Wiley-VCH Verlag GmbH & Co. KGaA, Weinheim

meric counterpart **4** in comparison with that of cyclophane **3** indicates the relatively intense π–π interaction between the two PDI rings in the former cyclophane. A similar conclusion can also be drawn by comparing the electrochemical properties of *trans* isomer **2a** and *cis* isomer **2b**.

Conclusion

A series of cyclophanes **1**–**3**, composed of two substituted PDI rings connected by two triazine spacers with rigid face-to-face dimeric structure, have been designed and prepared for the first time. In particular, the successful separation of the two isomers of cyclophane **2** has been achieved by TLC. The *trans* and *cis* isomers, **2a** and **2b**, were structurally characterized by 2D NMR spectroscopy. These cyclophanes with rigid face-to-face dimeric structures render it possible to correlate the molecular structure with optical and electrochemical properties. The structural parameters, including interplanar distance, lateral sideways slippage along the short or long axis of the PDI ring, and the in-plane torsion angle between the long axis of the PDI ring, seem to be the dominating factors that affect the optical or electrochemical properties definitively. Tiny structure differences will induce significant changes in the optical or electrochemical properties. To the best of our knowledge, this represents the first experimental effort towards understanding the correlation of the dimeric structure with the optical properties of PDI derivatives. The results will be useful for the design and preparation of new supramolecular systems of PDIs with novel structure and optical properties.

Experimental Section

General method: ^{1}H NMR spectra were recorded at 300 MHz with the solvent peak as internal standard (in $CDCl_3$). Electronic absorption spectra were recorded in organic solvents at room temperature. Fluorescence spectra and the fluorescence lifetime were measured on a multifrequency phase and modulation fluorometer with the excitation at 400 nm. The fluorescence lifetimes were measured by the multifrequency phase modulation method with a scattering sample as standard.[26] Fluorescence quantum yields were calculated with compound **4** as standard. MALDI-TOF mass spectra were obtained on an ultrahigh-resolution Fourier transform ion cyclotron resonance (FT-ICR) mass spectrometer. Electrochemical measurements were carried out under a nitrogen atmosphere on an electrochemical workstation. The cell comprised inlets for a glassy carbon disk working electrode 2.0 mm in diameter and a silver-wire counter electrode. The reference electrode was Ag/Ag^+, which was connected to the solution by a Luggin capillary, the tip of which was placed close to the working electrode. It was corrected for junction potentials by being referenced internally to the Fe^+/Fe couple [$E_{1/2}(Fe^+/Fe) = 501$ mV vs. SCE]. Typically, a solution (0.1 mol dm^{-3}) of $[Bu_4N][ClO_4]$ in dichloromethane containing the sample (0.5 mmol dm^{-3}) was purged with nitrogen for 10 min, then the voltammograms were recorded at ambient temperature. The scan rates were 20 and 10 mV s^{-1} for CV and DPV, respectively. TDDFT calculations with the B3LYP method and 6-31G(d) basis set were carried out to study the molecular structures, molecular orbitals, and electronic absorption spectra of these cyclophanes.

Materials: [*N*,*N*′-dicyclohexyl-1,7-di(*p*-*tert*-butylphenoxy)]perylene-3,4:9,10-tetracarboxylic diimide (**4**),[27] [*N*,*N*′-dicyclohexyl-1,7-di(piperidinyl)]perylene-3,4:9,10-tetracarboxylic diimide (**5**),[28] and [*N*,*N*′-dicyclohexyl-1,6,7,12-tetra(*p*-*tert*-butyl)phenoxy]perylene-3,4:9,10-tetracarboxylic diimide (**6**)[29] were prepared by following the literature methods. The dianhydrides **8**–**10** were prepared by the hydrolysis of compounds **4**–**6** in *n*-propanol and potassium hydroxide according to published procedures.[30] Other chemicals were purchased from commercial sources. Solvents were of analytical grade and purified by the standard method.

2-*N*,*N*-Di(*n*-butyl)amino-4,6-dihydrazine-1,3,5-triazine (7): A mixture of 2,4,6-trichloro-1,3,5-triazine (5.43 g, 29.4 mmol) and *N*,*N*′-diisopropylethylamine (DIPEA; 6 mL) in THF (40 mL) was cooled to 0–5 °C in a ice-water bath. Dibutylamine (4.99 mL, 29.4 mmol) was added dropwise in 30 min. The reaction mixture was stirred at 0–5 °C for another 30 min, then warmed to room temperature and kept at that temperature for 2 h. This reaction mixture was added slowly to a cooled mixture of THF (50 mL) and hydrazine (85%, 10 mL) at −10 °C. The resulting reaction mixture was further stirred at −10 °C for 6 h and then stirred continuously at room temperature for 24 h. After removing the solvent under reduced pressure, the residue was washed thoroughly with toluene, water, and methanol. Compound **7** was collected as a white solid (5.29 g, 67%). M.p. 122 °C; ^{1}H NMR (300 MHz, $CDCl_3$, 25 °C, TMS): $\delta = 6.52$ (br, 2H; NH), 4.23 (br, 4H; NCH_2), 3.48–3.56 (br, 4H; CH_2), 1.52–1.64 (br, 4H; CH_2), 1.30–1.40 (br, 4H; CH_2), 0.92 ppm (m, 6H; CH_3); MS (70 eV): *m*/*z* (%): 269.72 (100) [*M*+H]; elemental analysis calcd (%) for $C_{11}H_{24}N_8$: C 49.23, H 9.01, N 41.75; found: C 49.18, H 8.87, N 41.43.

Cyclophane 1: A mixture of [*N*,*N*′-dicyclohexyl-1,7-di(*p*-*tert*-butylphenoxy)]perylene-3,4:9,10-tetracarboxylic dianhydride (**8**; 88 mg, 0.129 mmol), imidazole (6 g), and 2-*N*,*N*-di(*n*-butyl)amino-4,6-dihydrazine-1,3,5-triazine (**7**; 35 mg, 0.129 mmol) in toluene (300 mL) was heated to reflux under a nitrogen atmosphere and kept at reflux for 48 h. The solvent was removed under reduced pressure and the residue was washed with dilute hydrochloric acid (10%, 100 mL) and then water. The product was purified by column chromatography on silica gel with chloroform as eluent. After recrystallization from chloroform and methanol, the product was collected as a red solid (9.8 mg, 8%). M.p. >300 °C; ^{1}H NMR (300 MHz, $CDCl_3$, 25 °C, TMS): $\delta = 9.54$ (d, J(H,H) = 8.1 Hz, 4H; perylene, isomer 1), 9.28 (d, J(H,H) = 8.4 Hz, 4H; perylene, isomer 2), 8.31 (d, J(H,H) = 8.1 Hz, 4H; perylene, isomer 1), 8.28 (d, J(H,H) = 8.4 Hz, 4H; perylene, isomer 2), 8.11 (s, 4H; perylene, isomer 2), 8.01 (s, 4H; perylene, isomer 1), 7.47 (m, 16H; phenyl, isomer 1+2), 7.07 (m, 16H; phenyl, isomer 1+2), 6.90 (s, 8H; NH, isomer 1+2), 3.52 (m, 16H; NCH_2, isomer 1+2), 1.62 (m, 16H; CH_2, isomer 1+2), 1.41–1.31 (m, 88H; CH_2+$C(CH_3)_3$, isomer 1+2), 0.96 ppm (t, 24H; CH_3, isomer 1+2); MS (MALDI-TOF): *m*/*z*: 1842.1 [M^+]; elemental analysis calcd (%) for $C_{110}H_{104}N_{16}O_{12}$: C 71.72, H 5.69, N 12.17; found: C 71.35, H 5.51, N 11.89.

Cyclophanes 2a and 2b: By using a similar procedure to that for preparing cyclophane **1**, with [*N*,*N*′-dicyclohexyl-1,6,7,12-tetra(*p*-*tert*-butyl)phenoxy]perylene-3,4:9,10-tetracarboxylic diimide (**10**; 127 mg, 0.129 mmol) instead of **8** as starting material, cyclophane **2** was synthesized. The product was purified by column chromatography on silica gel with chloroform as eluent. The first fraction contained cyclophanes **2a** and **2b**, which were further separated by preparative TLC. The first green fraction from TLC was **2a** (4 mg, 3.7%) and the second fraction was **2b** (1.3 mg, 1.2%).

2a: M.p. >300 °C; ^{1}H NMR (300 MHz, $CDCl_3$, 25 °C, TMS): $\delta = 9.66$ (d, J(H,H) = 8.4 Hz, 4H; perylene), 8.23 (s, 4H; perylene), 8.10 (d, J(H,H) = 8.4 Hz, 4H; perylene), 6.94 (s, 4H; NH), 3.61 (m, 8H; NCH_2), 3.21 (t, 4H; piperidine), 2.72 (d, 4H; piperidine), 2.17 (m, 8H; CH_2), 1.90 (m, 8H; CH_2), 1.69 (m, 16H; piperidine), 1.42 (m, 16H; piperidine), 0.98 ppm (t, 12H; CH_3); MS (MALDI-TOF): *m*/*z*: 1581.3 [M^+]; elemental analysis calcd (%) for $C_{90}H_{92}N_{20}O_8$: C 68.34, H 5.86, N 17.71; found: C 68.21, H 5.79, N 17.69.

2b: M.p. >300 °C; ^{1}H NMR (300 MHz, $CDCl_3$, 25 °C, TMS): $\delta = 9.84$ (d, J(H,H) = 8.4 Hz, 4H; perylene), 8.26 (s, 4H; perylene), 8.25 (d, J(H,H) = 8.4 Hz, 4H; perylene), 6.99 (s, 4H; NH), 3.58 (m, 8H; NCH_2), 3.23 (t, 4H; piperidine), 2.86 (m, 4H; piperidine), 2.35 (m, 8H; CH_2), 1.96 (m, 8H; CH_2), 1.65 (m, 16H; piperidine), 1.40 (m, 16H; piperidine), 1.03 ppm (t, 12H; CH_3); MS (MALDI-TOF): *m*/*z*: 1581.5 [M^+]; elemen-

 © 2008 Wiley-VCH Verlag GmbH & Co. KGaA, Weinheim

tal analysis calcd (%) for $C_{90}H_{92}N_{20}O_8$: C 68.34, H 5.86, N 17.71; found: C 68.12, H 5.85, N 17.69.

Cyclophane 3: By employing a similar procedure to that for cyclophane **1**, with [*N*,*N*′-dicyclohexyl-1,6,7,12-tetra(*p*-*tert*-butyl)phenoxy]perylene-3,4:9,10-tetracarboxylic diimide (**10**; 127 mg, 0.129 mmol) instead of **8** as starting material, cyclophane **3** was prepared. The product was purified by column chromatography on silica gel with chloroform as eluent. The first red fraction contained cyclophane **3** (5 mg, 3.1 %). M.p. >300 °C; ^{1}H NMR (300 MHz, $CDCl_3$, 25 °C, TMS): $\delta = 8.08$ (b, 4H; perylene), 7.88 (b, 4H; perylene), 7.08 (b, 16H; perylene), 6.80 (s, 4H; NH), 6.64 (b, 8H; phenyl), 6.41 (b, 8H; phenyl), 3.39 (b, 8H; NCH_2), 1.60–1.43 (m, 16H; CH_2), 1.20 (s, 72H; $C(CH_3)_3$), 0.92 ppm (t, 12H; CH_3); MS (MALDI-TOF): *m*/*z*: 2434.6 [*M*+H]; elemental analysis calcd (%) for $C_{151}H_{154}N_{16}O_{15}$: C 74.54, H 6.38, N 9.21; found: C 74.82, H 6.12, N 9.89.

Acknowledgements

Financial support from the Natural Science Foundation of China (Grant Nos. 20571049, 20771066, 20431010), Ministry of Education of China, and Shandong University is gratefully acknowledged.

[1] M. R. Wasielewski, *Chem. Rev.* **1992**, *92*, 435–461.
[2] M. Gust, T. A. Moore, A. L. Moore, *Acc. Chem. Res.* **2001**, *34*, 40–48.
[3] J. A. A. W. Elemans, R. van Hameren, R. J. M. Nolte, A. E. Rowan, *Adv. Mater.* **2006**, *18*, 1251–1266.
[4] M. D. Ward, *Chem. Soc. Rev.* **1997**, *26*, 365–375.
[5] J.-M. Lehn, *Science* **2002**, *295*, 2400–2403.
[6] G. M. Whitesides, J. P. Mathias, C. T. Seto, *Science* **1991**, *254*, 1312–1319.
[7] a) Z. Wang, C. J. Medforth, J. A. Shelnutt, *J. Am. Chem. Soc.* **2004**, *126*, 15954–15955; b) R. Takahashi, Y. Kobuke, *J. Am. Chem. Soc.* **2003**, *125*, 2372–2373; c) D. Furutsu, A. Satake, Y. Kobuke, *Inorg. Chem.* **2005**, *44*, 4460–4462; d) O. Shoji, H. Tanaka, T. Kaway, Y. Kobuke, *J. Am. Chem. Soc.* **2005**, *127*, 8598–8599; e) R. F. Kelley, W. S. Shin, B. Rybtchinski, L. E. Sinks, M. R. Wasielewski, *J. Am. Chem. Soc.* **2007**, *129*, 3173–3181.
[8] a) X. Li, L. E. Sinks, B. Rybtchinski, M. R. Wasielewski, *J. Am. Chem. Soc.* **2004**, *126*, 10810–10811; b) P. Samori, H. Engelkamp, P. A. J. de Witte, A. E. Rowan, R. J. M. Nolte, J. P. Rabe, *Adv. Mater.* **2005**, *17*, 1265–1268; c) P. Samori, H. Engelkamp, P. de Witte, A. E. Rowan, R. J. M. Nolte, J. P. Rabe, *Angew. Chem.* **2001**, *113*, 2410–2412; *Angew. Chem. Int. Ed.* **2001**, *40*, 2348–2350; d) J. Sly, P. Kasak, E. Gomar-Nadal, C. Rovia, L. Gorriz, P. Thordarson, D. B. Amabilino, A. E. Rowan, R. J. M. Nolte, *Chem. Commun.* **2005**, 1255–1257; e) A. de la Escosura, M. V. Martinez-Diaz, P. Thordarson, A. E. Rowan, R. J. M. Nolte, T. Torres, *J. Am. Chem. Soc.* **2003**, *125*, 12300–12308.
[9] a) O. J. Dautel, G. Wantz, R. Almairac, D. Flot, L. Hirsch, J.-P. Lere-Porte, J.-P. Parneix, F. Serein-Spirau, L. Vignau, J. J. E. Moreau, *J. Am. Chem. Soc.* **2006**, *128*, 4892–4901; b) T. Ishi-i, K. Yaguma, R. Kuwahara, Y. Taguri, S. Mataka, *Org. Lett.* **2007**, *8*, 585–588; c) W. Pisula, Z. Tomovic, C. Simpson, M. Kastler, T. Pakula, K. Müllen, *Chem. Mater.* **2005**, *17*, 4296–4303; d) E. H. A. Beckers, S. C. J. Meskers, A. P. H. J. Schenning, Z. Chen, F. Würthner, P. Marsal, D. Beljonne, J. Cornil, R. A. J. Janssen, *J. Am. Chem. Soc.* **2006**, *128*, 649–657; e) A. Lohr, M. Lysetska, F. Würthner, *Angew. Chem.* **2005**, *117*, 5199–5202; *Angew. Chem. Int. Ed.* **2005**, *44*, 5071–5074; f) M. R. Wasielewski, *J. Org. Chem.* **2006**, *71*, 5051–5066.
[10] a) B. A. Jones, M. J. Ahrens, M.-H. Yoon, A. Facchetti, T. J. Marks, M. R. Wasielewski, *Angew. Chem.* **2004**, *116*, 6523–6526; *Angew. Chem. Int. Ed.* **2004**, *43*, 6363–6366; b) Z. Chen, M. G. Debije, T. Debaerdemaeker, P. Osswald, F. Würthner, *ChemPhysChem* **2004**, *5*, 137–140; c) P. Jonkheijm, N. Stutzmann, Z. Chen, D. M. de Leeuw, E. W. Meijer, A. P. H. J. Schenning, F. Würthner, *J. Am. Chem. Soc.* **2006**, *128*, 9535–9540; d) P. R. L. Malenfant, C. D. Dimitrakopoulos, J. D. Gelorme, L. L. Kosbar, T. O. Graham, *Appl. Phys. Lett.* **2002**, *80*, 2157–2519.
[11] a) B. A. Gregg, R. A. Cormier, *J. Am. Chem. Soc.* **2001**, *123*, 7959–7960; b) A. J. Breeze, A. Salomon, D. S. Ginley, B. A. Gregg, H. Tillmann, H. H. Horhold, *Appl. Phys. Lett.* **2002**, *81*, 3085–3087; c) B. A. Gregg, *J. Phys. Chem.* **1996**, *100*, 852–859; d) C.-C. You, C. R. Saha-Möller, F. Würthner, *Chem. Commun.* **2004**, 2030–2031; e) J. Hua, F. Meng, F. Ding, F. Li, H. Tian, *J. Mater. Chem.* **2004**, *14*, 1849–1853; f) E. E. Neuteboom, P. A. van Hal, R. A. J. Janssen, *Chem. Eur. J.* **2004**, *10*, 3907–3918.
[12] a) M. A. Angadi, D. Gosztola, M. R. Wasielewski, *Mater. Sci. Eng. B* **1999**, *63*, 191–194; b) P. Ranke, I. Bleyl, J. Simmerer, D. Haarer, A. Bacher, H. W. Schmidt, *Appl. Phys. Lett.* **1997**, *71*, 1332–1334; c) S. Alibert-Fouet, S. Dardel, H. Bock, M. Oukachmih, S. Archambeau, I. Seguy, P. Jolinat, P. Destruel, *ChemPhysChem* **2003**, *4*, 983–985; d) P. Schouwink, A. H. Schafer, C. Seidel, H. Fuchs, *Thin Solid Films* **2000**, *372*, 163–168; e) T. Zukawa, S. Naka, H. Okada, H. Onnagawa, *J. Appl. Phys.* **2002**, *91*, 1171–1174.
[13] T. van der Boom, R. T. Hayes, Y. Zhao, P. J. Bushhard, E. A. Weiss, M. R. Wasielewski, *J. Am. Chem. Soc.* **2002**, *124*, 9582.
[14] J. M. Giaimo, A. V. Gusev, M. R. Wasielewski, *J. Am. Chem. Soc.* **2002**, *124*, 8530–8531.
[15] a) W. Wang, J. J. Han, L. Q. Wang, L. S. Li, W. J. Shaw, A. D. Q. Li, *Nano Lett.* **2003**, *3*, 455–458; b) W. Wang, W. Wan, H. H. Zhou, S. Niu, A. D. Q. Li, *J. Am. Chem. Soc.* **2003**, *125*, 5248–5249; c) W. Wang, L. S. Li, G. Helms, H. H. Zhou, A. D. Q. Li, *J. Am. Chem. Soc.* **2003**, *125*, 1120–1121.
[16] Y. Wang, Y. Chen, R. Li, S. Wang, W. Su, P. Ma, M. R. Wasielewski, X. Li, J. Jiang, *Langmuir* **2007**, *23*, 5836–5842.
[17] H. Langhals, R. Ismael, *Eur. J. Org. Chem.* **1998**, 1915–1917.
[18] A. E. Clark, C. Qin, A. D. Q. Li, *J. Am. Chem. Soc.* **2007**, *129*, 7586–7595.
[19] a) C. Zhao, R. Li, X. Li, J. Jiang, *J. Org. Chem.* **2007**, *72*, 2402–2410; b) C.-C. Chao, M.-K. Leung, O. Y. Su, K.-Y. Chiu, T.-H. Lin, S.-J. Shieh, S.-C. Lin, *J. Org. Chem.* **2005**, *70*, 4323–4331.
[20] X. Li, J. Illigen, M. Nieger, S. Michel, C. A. Schalley, *Chem. Eur. J.* **2003**, *9*, 1332–1347.
[21] a) Z. Chen, U. Baumeister, C. Tschierske, F. Würthner, *Chem. Eur. J.* **2007**, *13*, 450–465; b) Z. Chen, V. Stepanenko, V. Dehm, P. Prins, L. D. A. Siebbeles, J. Seibt, P. Marquetand, V. Engel, F. Würthner, *Chem. Eur. J.* **2007**, *13*, 436–449; c) F. Würthner, C. Thalacker, S. Diele, C. Tschierske, *Chem. Eur. J.* **2001**, *7*, 2245–2253.
[22] Gaussian 03, Revision B.05, M. J. Frisch, G. W. Trucks, H. B. Schlegel, G. E. Scuseria, M. A. Robb, J. R. Cheeseman, J. A. Montgomery, Jr., T. Vreven, K. N. Kudin, J. C. Burant, J. M. Millam, S. S. Iyengar, J. Tomasi, V. Barone, B. Mennucci, M. Cossi, G. Scalmani, N. Rega, G. A. Petersson, H. Nakatsuji, M. Hada, M. Ehara, K. Toyota, R. Fukuda, J. Hasegawa, M. Ishida, T. Nakajima, Y. Honda, O. Kitao, H. Nakai, M. Klene, X. Li, J. E. Knox, H. P. Hratchian, J. B. Cross, C. Adamo, J. Jaramillo, R. Gomperts, R. E. Stratmann, O. Yazyev, A. J. Austin, R. Cammi, C. Pomelli, J. W. Ochterski, P. Y. Ayala, K. Morokuma, G. A. Voth, P. Salvador, J. J. Dannenberg, V. G. Zakrzewski, S. Dapprich, A. D. Daniels, M. C. Strain, O. Farkas, D. K. Malick, A. D. Rabuck, K. Raghavachari, J. B. Foresman, J. V. Ortiz, Q. Cui, A. G. Baboul, S. Clifford, J. Cioslowski, B. B. Stefanov, G. Liu, A. Liashenko, P. Piskorz, I. Komaromi, R. L. Martin, D. J. Fox, T. Keith, M. A. Al-Laham, C. Y. Peng, A. Nanayakkara, M. Challacombe, P. M. W. Gill, B. Johnson, W. Chen, M. W. Wong, C. Gonzalez, J. A. Pople, Gaussian, Inc., Pittsburgh PA, **2003**.
[23] M. Kasha, H. R. Rawls, M. A. El-Bayoumi, *Pure Appl. Chem.* **1965**, *11*, 371–392.
[24] M. J. Ahrens, L. E. Sinks, B. Rybtchinski, W. Liu, B. A. Jones, J. M. Giaimo, A. V. Gusev, A. J. Goshe, D. M. Tiede, M. R. Wasielewski, *J. Am. Chem. Soc.* **2004**, *126*, 8284–8394.
[25] a) R. L. Fulton, M. Gouterman, *J. Chem. Phys.* **1964**, *41*, 2280–2286; b) L. Oddos-Marcel, F. Madeore, A. Bock, D. Neher, A. Ferencz, H.

 © 2008 Wiley-VCH Verlag GmbH & Co. KGaA, Weinheim

Rengel, G. Wegner, C. Kryschi, H. P. Trommsdorff, *J. Phys. Chem.* **1996**, *100*, 11850–11856.
[26] a) A. R. Dunn, I. J. Dmochowski, J. R. Winkler, H. B. Gray, *J. Am. Chem. Soc.* **2003**, *125*, 12450–12456; b) B. Mysliwa-Kurdziel, J. Kruk, K. Strzalka, *Photochem. Photobiol.* **2004**, *79*, 62–67.
[27] M. J. Ahrens, M. J. Tauber, M. R. Wasielewski, *J. Org. Chem.* **2006**, *71*, 2107–2114.
[28] Y. Zhao, M. R. Wasielewski, *Tetrahedron Lett.* **1999**, *40*, 7047–7050.
[29] F. Würthner, C. Thalacker, A. Sautter, W. Schärtl, W. Ibach, O. Hollricher, *Chem. Eur. J.* **2000**, *6*, 3871–3886.
[30] L. E. Sinks, B. Rybtchinski, M. Iimura, B. A. Jones, A. J. Goshe, X. Zuo, D. M. Tiede, X. Li, M. R. Wasielewski, *Chem. Mater.* **2005**, *17*, 6295–6303.

Received: January 23, 2008
Revised: May 12, 2008
Published online: July 4, 2008

 © 2008 Wiley-VCH Verlag GmbH & Co. KGaA, Weinheim